

Supporting Information

Grigoryan et al. 10.1073/pnas.1310490110

SI Methods

Transgenic and Mutant Mice. All animal experiments were conducted in accordance with national, European and internal MDC regulations. Genotypes were determined by PCR on genomic DNA derived from ear biopsies or yolk sacs. Phenotypes were analyzed on a mixed C57BL6/129 background.

Antibodies, Chemical Inhibitors, and Wnt/Rspondin Ligands. The following antibodies were used: anti-neurofilament, anti-vinculin, and anti- α -tubulin (Sigma-Aldrich); anti-S100 (Dako); anti- β -catenin (1); anti-BrDU and anti-YFP (Upstate); anti-Ki67 (Abcam); anti-E-cadherin and anti-N-cadherin (Becton Dickinson); anti-Mag and anti-Cldn5 (Acris); anti-myelin basic protein and anti-Krox20 (Santa Cruz Biotechnology); anti-cMaf (produced by Hagen Wende); anti-Sox2 (Novus Biologicals); and anti-L1 (a gift from Fritz Rathjen, Max Delbrück Centrum for Molecular Medicine, Berlin, Germany). Secondary antibodies were conjugated with Cy2, Cy3, or Cy5 fluorochromes (Jackson ImmunoResearch Laboratories) or with peroxidase (Dianova). Phalloidin was rhodamine-conjugated (Sigma-Aldrich). The following signaling inhibitors were used: Chir98014 (Axon MedChem), Y27632 and SB203580 (Sigma-Aldrich), NSC23766 (Tocris Bioscience), and TAE226 (generously provided by Novartis Pharma AG). For spreading assays, cells were pretreated for 20 h with the inhibitors, which were also present during the assay. Wnt3a ligand was purchased from R&D Systems. Rspondin 2 and 3 were either from R&D Systems or produced by overexpressing alkaline-phosphatase-tagged Rspondin 2 or 3 in HEK293 cells, as described (2, 3). Statistical analysis was performed with SPSS16.0. Galactosidase assays were performed on cryosections as previously described (4).

Cell Culture, Flow Cytometry, and Teased Fiber Preparation. Schwann cells (SCs) were isolated from E13.5 dorsal root ganglia as described (5). For proliferation assays, cells were grown in the presence of 30 μ M BrdU for 20 h, fixed in 4% formaldehyde in PBS, and treated with 2.4 M HCl at 37 °C for 20 min before immunolabeling. For migration experiments, SCs were grown to confluence and treated with 10 μ M Mitomycin C for 2 h to prevent further proliferation. Scratch wounds in cell monolayers were performed 1 d after Mitomycin C treatment using a 200- μ L pipette tip. The scratched area was photographed at 0, 24, and 48 h. For flow cytometry analysis, 10⁶ cells were fixed in ice-cold 70% ethanol; washed with PBS; and stained with 20 μ M Propidium iodide solution, which contained 200 μ M RNase A. The cell cycle stages were determined by measuring amounts of DNA with a LSRII Flow Cytometer (Becton Dickinson) and were analyzed with FlowJo software (Tree Star). For the teased fiber preparations, sciatic nerves of 6-wk-old mice were fixed with 4% formaldehyde, washed in PBS, and teased on positively charged glass slides (Superfrost Plus; Thermo Scientific).

Western Blotting. Cultured SCs were lysed in radioimmunoprecipitation assay (RIPA) buffer and Hepes/TritonX-100 buffer, which contained protease inhibitor mixture (Roche) and 1 mM sodium orthovanadate. Total protein (20 μ g) was separated in acrylamide gels and transferred to PVDF membranes (Millipore). For detection of antibodies, an ECL kit (Amersham) was used. Intensity of the bands was quantified using VilberLumat Fusion SL software.

RNA Preparation and Quantitative Real-Time PCR. Sciatic nerves or cells were processed for RNA isolation using TRIzol reagent (Invitrogen). Reverse transcription was performed using 2–5 μ

RNA, oligo (dT) primers, and Moloney murine leukemia virus reverse transcriptase (New England Biolaboratories). Quantitative PCR was performed on a LightCycler (BioRad), according to the manufacturer's instructions, using the Absolute quantitative real-time PCR (qRT-PCR) SYBR Green mix (Thermo Fisher Scientific). The following primers were used: Wnt1 fwd 5'-AGTCCTGCACCTGCGACTAC-3'; Wnt1 rev 5'-CTTGGCGCATCTCAGAGAAC-3'; Wnt2 fwd 5'-TCTTCAGCTGGCGTTGTATTTGCC-3'; Wnt2 rev 5'-GTTGTTGTAGAGTTTCATCAGGGC-3'; Wnt2b fwd 5'-CACCCGACCTGATCTTGTCT-3'; Wnt2b rev 5'-TGTTTTCTGCACCTTGCAC-3'; Wnt3 fwd 5'-TCCACTGGTGTGCTATGTC-3'; Wnt3rev 5'-AACAGTCCATGCTCCTTGCT-3'; Wnt3a fwd 5'-TTTGGAGGAATGGTCTCTCG-3'; Wnt3a rev 5'-ACCACCAGCAGGTCTTCACT-3'; Wnt5a fwd 5'-GTGCCATGTCTTCCAAGTTCTTCC-3'; Wnt5a rev 5'-TGCATGTGGTCTGATCAACAGTG-3'; Wnt5b fwd 5'-TCAGAGAGTGGCAACACCAG-3'; Wnt5b rev 5'-AGCCGTACTCCAGTTGTCT-3'; Wnt6 fwd 5'-TTCGGGGATGAGAAGTCAAG-3'; Wnt6 rev 5'-AAAGCCATGGCACTTACAC-3'; Wnt9b fwd 5'-TTTAAGGAGACGGCCTTCTGTATGC-3'; Wnt9b rev 5'-TTCAGATTGTCACACACACACCC-3'; Wnt11 fwd 5'-ATATCCGGCTGTGAAGGACTCAG-3'; Wnt11 rev 5'-ACCAGTGGTACTTGCAGTGCATC-3'; R1 fwd 5'-CTGGTTCTGAGTGGACACA-3'; R1 rev 5'-GTGCTCGATCTTGCATTTGA-3'; R2 fwd 5'-GAAACGAGAACACGGCAGAT-3'; R2 rev 5'-TGCTCTTGGGCTCTCTCAAT-3'; R3 fwd 5'-ATCCTTACGCCAAGGGTAA-3'; R3 rev 5'-CAATGCTGGACTCCAAACCT-3'; R4 fwd 5'-TGGA-GTCCCTGCATACACAA-3'; R4 rev 5'-CCAACTTCTGTCTTACGC-3'; Fzd1 fwd 5'-TGGTTTTAGCCAAACTGCA-A-3'; Fzd1 rev

5'-CCAGACAGGAGCACACAAGA-3'; Fzd2 fwd 5'-GGTGGGGTTGAGTGTTTACG-3'; Fzd2 rev 5'-TCTGGCACACTGGTCTTACG-3'; Fzd3 fwd 5'-GCTCCAGGAACCTGACTTTG-3'; Fzd3 rev 5'-ATGCTGCCGTGAGGTAGTCT-3'; Fzd4 fwd 5'-AACCTCGGCTACAACGTGAC-3'; Fzd4 rev 5'-TG-GCATAAAACCGAACAAA-3'; Fzd5 fwd 5'-GAAGGAAGA-GAAGGCGAGTG-3'; Fzd5 rev 5'-ATAGGGCTGGAGGGAT-GATT-3'; Fzd6 fwd 5'-CACAAATCATGGCACCTCTG-3'; Fzd6 rev 5'-GTCTCAGGAACGCTGCTCTT-3'; Fzd7 fwd 5'-GCATCATGGGAGTTGACCTT-3'; Fzd7 rev 5'-CACAAA-AGATGCCAAACCTG-3'; Fzd8 fwd 5'-GTTTTTGCACCTTCCCAA-3'; Fzd8 rev 5'-GCTCTGTAAAGGCGACTG-C-3'; Fzd9 fwd 5'-TTATGGTTGCTCCCTCCTTG-3'; Fzd9 rev 5'-CACTCCCTGCATGAGACAGA-3'; Fzd10 fwd 5'-ACA-TTTTCCCCCTCTCCCTA-3'; Fzd10 rev 5'-CCCTTCTCTCC-ACAAATCA-3'; LGR4 fwd 5'-AGATAACAGCCCCCAAGA-CC-3'; LGR4 rev 5'-GCAGGCAGTGATGAACAAGA-3'; LGR5 fwd 5'-TAAAGACGCGCAACAGTG-3'; LGR5 rev 5'-GATTTCGGATCAGCCAGCTAC-3'; LGR6 fwd 5'-GTGCC-AGCTTCTTCAAGACC-3'; LGR6 rev 5'-CCAGCTCTCAAA-GAGGTGCT-3';

INTA4 fwd 5'-GACCCAAACGACATTTACC-3'; INTA4 rev 5'-CGGGTCTTCTGAACAGGATT-3'; Cdh2 fwd 5'-GAGAGGCTATCCATGCTGA-3'; Cdh2 rev

5'-CGCTACTGGAGGAGTTGAGG-3'; Ncam fwd 5'-AGA-CAAGCCTTTGCCTTTGA-3'; Ncam rev 5'-GTAAGTCCCATGTACCTT-3'; P75 fwd 5'-GGAACAGCTGCAAGCA-AAAT-3'; P75 rev 5'-CAGCTTCTGACCTCCTCAC-3'; GAP43 fwd 5'-AGCCAAGGAGGAGCCTAAAC-3'; GAP43 rev 5'-CTGTGGGCACTTTCTTCTAG-3'; Sox2 fwd 5'-ATGGG-CTCTGTGGTCAAGTC-3'; Sox2 rev 5'-CCCTCCCAATT-

CCCTTGAT-5'; Galc fwd 5'-CATGCGGACGTTACAGC-TAA-3'; Galc rev 5'-AGGATCCAGCAAAAATGCAC-3'; Pmp22 fwd 5'-TCCTCATCAGTGAGCGAATG-3'; Pmp22 rev 5'-ATGTAGGCGAAGCCATAGGA-3'; P0 fwd 5'-GGCAAGACCTC-TCAGGTCAC-3'; P0 rev 5'-CCCAGCCCTTTTGATTTCTT-3'; Prx fwd 5'-GGACGGTGTCTGGATACGAG-3'; Prx rev 5'-GCTCTAACTGAGGGGCTGTG-3'; Olig1 fwd 5'-GGTTCCGAGCTGGATGTTA-3'; Olig1 rev 5'-AGCAAGCTCAAACGTTGGTT-3'; Fgf5 fwd 5'-GCTGTGTCTCAGGGGATTGT-3'; Fgf5 rev 5'-GAAGTGGTGGAGACGTGTT-3'; Shh fwd 5'-TTAAATGCCTTGCCATCTC-3'; Shh rev 5'-GGGACGTAAGTCCTCACCA-3'; EphA5 fwd 5'-CGTCAACATGCTGGACAAAC-3'; EphA5 rev 5'-CCGTTTACCATCTGCACCTT-3'; Ecgr4

fwd 5'-CTGTAGCCGAGAACACAGCA -3'; Ecgr4 rev 5'-GTAGTCATGGCCGTTTCGAT -3'; Dnajc6 fwd 5'-CCTCAGAACC-GACCCAATTA-3'; Dnajc6 rev 5'-TTGCCCTCTATCCACTC-CAG-3'; Aldh1a3 fwd 5'-AATGTCTGGGAATGGCAGAG-3'; Aldh1a3 rev 5'-AAAGCATGCGTGTGAGTGAG-3'; Jun fwd 5'-GGAGGGGTTACAAACTGCAA-3'; Jun rev 5'-TACAAA-CATCGGGCAGGACA-3'

Nkd1 fwd 5'-CATTGCGTGGATGAGAACAT-3'; Nkd1 rev 5'-GTGTCAAGGAGGTGGAAGGA-3'; GFAP fwd 5'-CACGAACGAGTCCCTAGAGC-3'; GFAP rev 5'-CTTCCCCTTC-TTTGGTGCTT-3'; Axin2 fwd 5'-AGTCAGCAGAGGGACA-GGAA-3'; Axin2 rev 5'-CTTCGTACATGGGGAGCACT-3'

- Huelsken J, Vogel R, Erdmann B, Cotsarelis G, Birchmeier W (2001) beta-Catenin controls hair follicle morphogenesis and stem cell differentiation in the skin. *Cell* 105(4):533–545.
- Glinka A, et al. (2011) LGR4 and LGR5 are R-spondin receptors mediating Wnt/ β -catenin and Wnt/PCP signalling. *EMBO Rep* 12(10):1055–1061.
- Ohkawara B, Glinka A, Niehrs C (2011) Rspo3 binds syndecan 4 and induces Wnt/PCP signaling via clathrin-mediated endocytosis to promote morphogenesis. *Dev Cell* 20(3): 303–314.
- Hogan BL, Beddington R, Constantini F, Lacy E (1994) *Manipulating the Mouse Embryo* (Cold Spring Harbor Laboratory Press, Cold Spring Harbor, NY).
- Woodhoo A, Dean CH, Droggiti A, Mirsky R, Jessen KR (2004) The trunk neural crest and its early glial derivatives: A study of survival responses, developmental schedules and autocrine mechanisms. *Mol Cell Neurosci* 25(1):30–41.

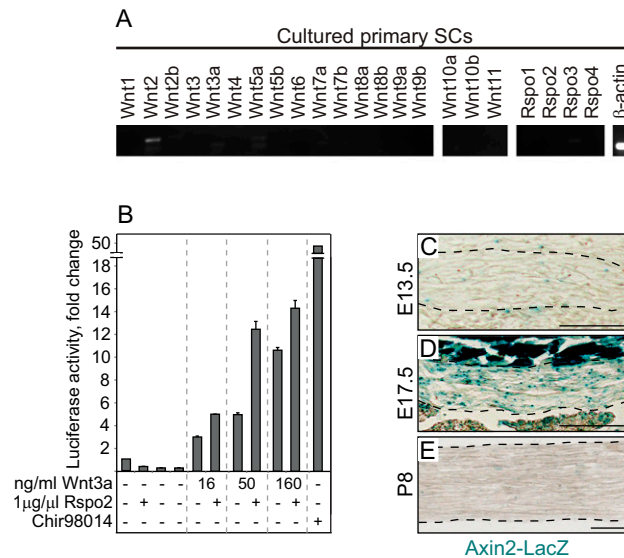


Fig. S1. Expression of Wnt pathway components and activity of Wnt signaling during SC development. (A) Analysis of the expression of components of canonical Wnt signaling by quantitative real-time PCR in primary SC cultures. (B) Synergistic coactivation of canonical Wnt signaling by Wnt3a and Rspo2 determined by activity of the Wnt-reporter Topflash in the RT4 cell line. Treatment with Chir98014, a pharmacological inhibitor of GSK3 and activator of Wnt signaling, was used as a positive control. (C–E) The Wnt-reporter Axin2-LacZ mice show β -Galactosidase activity in the sciatic nerves at different stages. Contours of the sciatic nerves are indicated with dashed lines. The dark blue staining at E17.5 represents high β -Galactosidase activity in the surrounding muscle. (Scale bars: 100 μ m in C and D and 500 μ m in E.) Errors bars represent SD ($n = 4$).

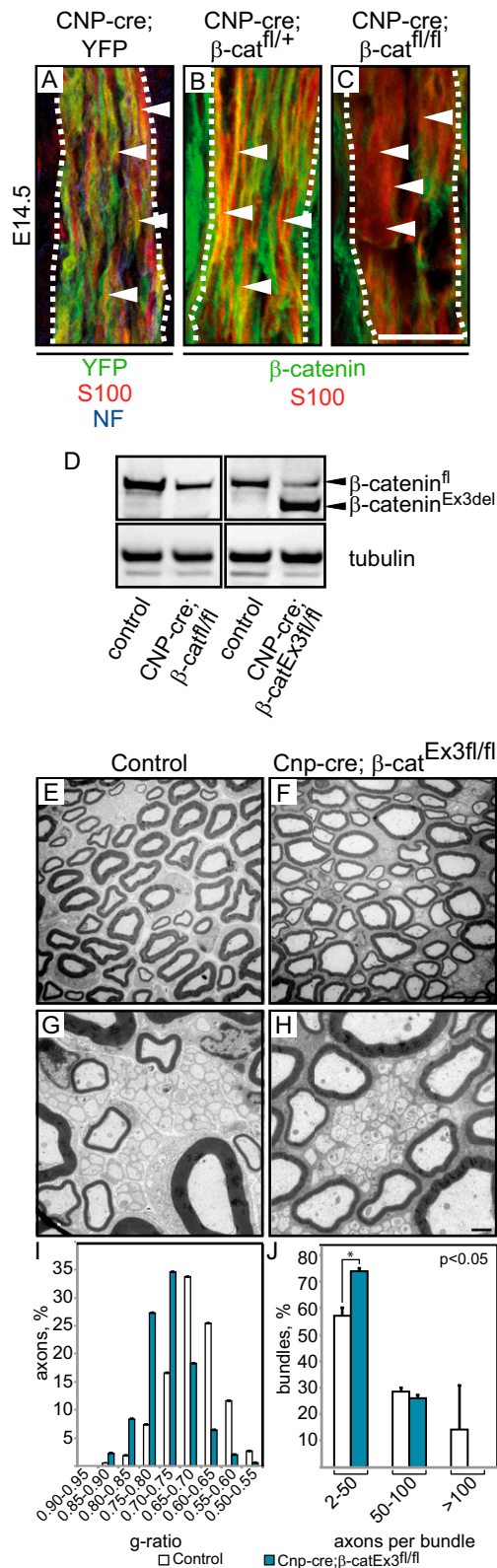


Fig. S2. Cnp-cre induced recombination of β -catenin in SCs and hypomyelination in β -catenin^{Ex3fl/fl} mutant mice. (A–C) Immunostainings were performed on longitudinal sections of embryonic sciatic nerves and depict recombination of (A) a YFP-reporter allele and (B and C) the β -catenin^{fl/fl} allele, using antibodies against S100 (red), YFP (green), β -catenin (green), and neurofilament (blue). Dashed contours outline the sciatic nerves. (Scale bar: 25 μ m.) (D) Analysis of β -catenin protein levels by Western blotting. Extracts of sciatic nerves from control, Cnp-cre; β -catenin^{fl/fl}, and Cnp-cre; β -catenin^{Ex3fl/fl} mice at P1 were analyzed; α -tubulin served as a loading control. Note an up-regulation of a shorter band corresponding to the constitutively active β -catenin protein, which lacks sequences encoded by exon 3. (E–H) Electron microscopic analysis of (E and G) control and (F and H) Cnp-cre; β -cat^{Ex3fl/fl} mice show a marked hypomyelination at p25. (Scale bar: 1 μ m.) (I) Quantification of the g ratios in control (white) and Cnp-cre; β -cat^{Ex3fl/fl} (blue) mice. Shown are the percentages of axons that display a particular g ratio. (J) Quantification of axonal bundles in the control (white) and Cnp-cre; β -cat^{Ex3fl/fl} (blue) mice. Shown is the percentage of bundles that contain a particular range of numbers of axons. Errors bars indicate SD calculated from two control and three mutant mice.

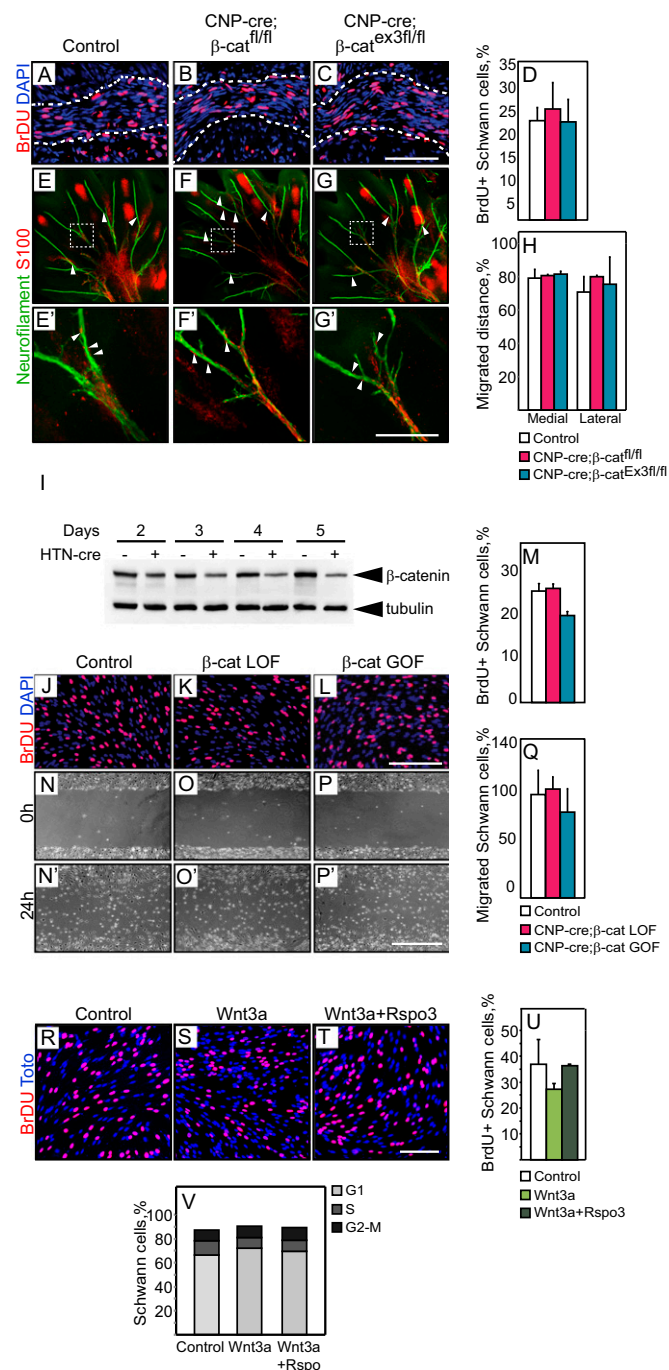


Fig. S3. Proliferation and migration of β -catenin mutant SCs in vivo and in vitro. (A–D) Proliferation of the SCs of indicated genotypes in vivo. (A–C) Longitudinal sections of embryonic sciatic nerves at E17.5 were assessed by measuring the rate of BrdU incorporation with immunohistochemistry using antibodies against BrdU and the nuclear counterstain DAPI. (D) Quantification of proliferation. Shown is the percentage of SCs that incorporated BrdU. (E–H) Migration of SCs of indicated genotypes in vivo. (E–G) Whole-mount immunostaining of E14.5 embryonic hindlimbs for the neuronal marker neurofilament (green) and the SC marker S100 (red) to visualize migrating cells in vivo. (H) Quantification of SC migration was performed by measuring the parts of nerves covered by SCs. Migration was quantified on hindlimbs by measuring the nerve length from the bifurcation of medial plantar (*Left*) and lateral plantar (*Right*) nerves to the tips. The total amount of SCs in this experiment could not be compared directly due to the potentially variable antibody penetrance at E14.5. (I–V) Proliferation and migration of β -catenin mutant SCs in vitro. β -catenin loss-of-function (LOF) mutations were introduced by treating primary cell cultures with HTN-cre, and gain-of-function (GOF) mutations were mimicked by adding Chir98014, a pharmacological inhibitor of GSK3 β and Wnt activator. (I) Loss of β -catenin protein in primary cell cultures 2–5 d after HTN-cre–induced in vitro recombination. As controls, HTN-cre–treated β -catenin^{fl/+} or untreated β -catenin^{fl/fl} cells were used. (J–L) Proliferation of the SCs of indicated genotypes assessed by measuring the rate of BrdU incorporation with immunohistochemistry using antibodies against BrdU and the nuclear counterstain DAPI. (M) Quantification of proliferation. Shown is the percentage of SCs that incorporated BrdU. (N–P) Migration in vitro was addressed by measuring migration of the SCs into the scratched wound area after 24 h. (Q) Quantification of SC migration, assessed by the percentage of SCs that migrated into the scratched area (as control, HTN-cre–treated β -catenin^{fl/+} or untreated β -catenin^{fl/fl} cells were used). (R–T) Proliferation of SCs upon treatment with Wnt3a alone or in combination with Rspo3, as assessed by measuring the rate of BrdU incorporation by immunohistochemistry using antibodies against BrdU and nuclear counterstain DAPI. (U) Quantification of proliferation. Shown is the percentage of SCs that incorporated BrdU. (V) Percent

Legend continued on following page

tages of cells in the G1, S, and G2-M phases of the cell cycle, after treatment with Wnt3a or combination of Wnt3a and Rspo3, as determined by labeling the cells with Propidium iodide and analyzing the amount of labeled DNA by flow cytometry. Error bars indicate SD calculated from three independent experiments or from at least three mice per group. (Scale bars: 100 μ m.)

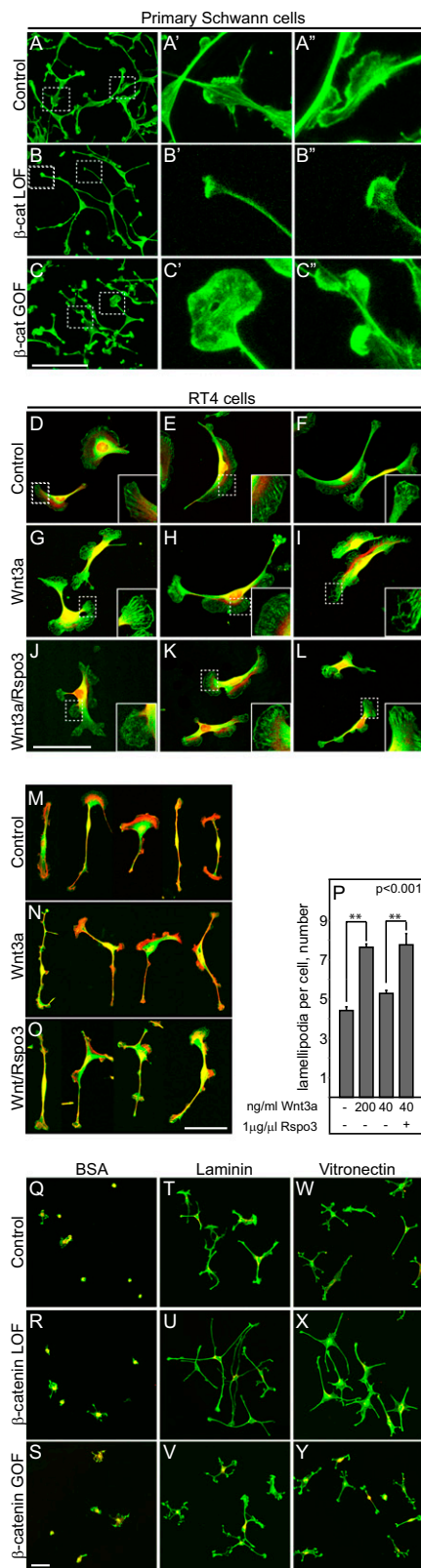


Fig. 54. Cell spreading and lamellipodia formation in the β -catenin mutant SCs and lamellipodia induction in the SCs and RT4 cells by Wnt3a and Rspo3. (A–C) SC shape and lamellipodia formation were analyzed by immunostaining using antibodies against vinculin. SCs carrying β -catenin LOF mutations fail to produce terminal lamellipodia, whereas SCs mimicking β -catenin GOF mutations produce more lamellipodia. (D–L) Lamellipodia formation in RT4 cells in the absence and presence of Wnt3a and Rspo3 ligands as assessed by immunostaining using Phalloidin (red) and antibodies against vinculin (green). (M–O) Immunostaining for vinculin (green) and staining for actin [Phalloidin (red)] reveals that treatment of primary mouse SCs with Wnt3a or a combination of low-dosage Wnt3a and Rspo3 induces lamellipodia formation. (P) Quantification of the lamellipodia in M–O. Shown is the average number of lamellipodia per cell.

Legend continued on following page

Error bars indicate SEM. (Scale bars: 40 μm .) *t* test: $^{**}P < 0.01$. (Q–Y) Staining for actin [Phalloidin (red)] and using antibodies against vinculin (green) on (T–V) laminin and (W–Y) vitronectin for the genotypes indicated. (Q–S) BSA coating was used as control for near absence of spreading. (Scale bars: 15 μm .)

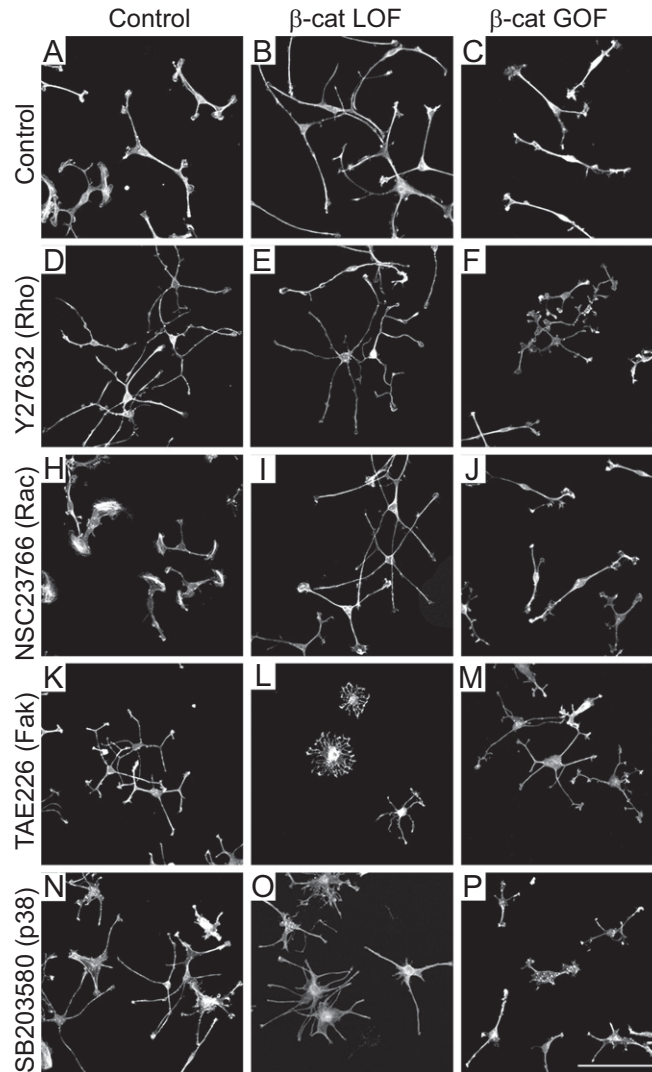


Fig. S5. Lamellipodia formation in the β -catenin LOF and GOF primary SCs in the presence of pharmacological inhibitors of Rho, Rac, FAK, and p38. Control, β -catenin LOF, and β -catenin GOF SCs that spread on laminin were treated with (A–C) DMSO, (D–F) Rho inhibitor Y27632, (H–J) Rac inhibitor NSC23766, (K–M) FAK inhibitor TAE226, or (N–P) p38 inhibitor SB03580. Each of the treatments imposed additional changes in cell morphology but was not able to rescue lamellipodia formation in β -catenin LOF or GOF cells. (Scale bar: 100 μm .)

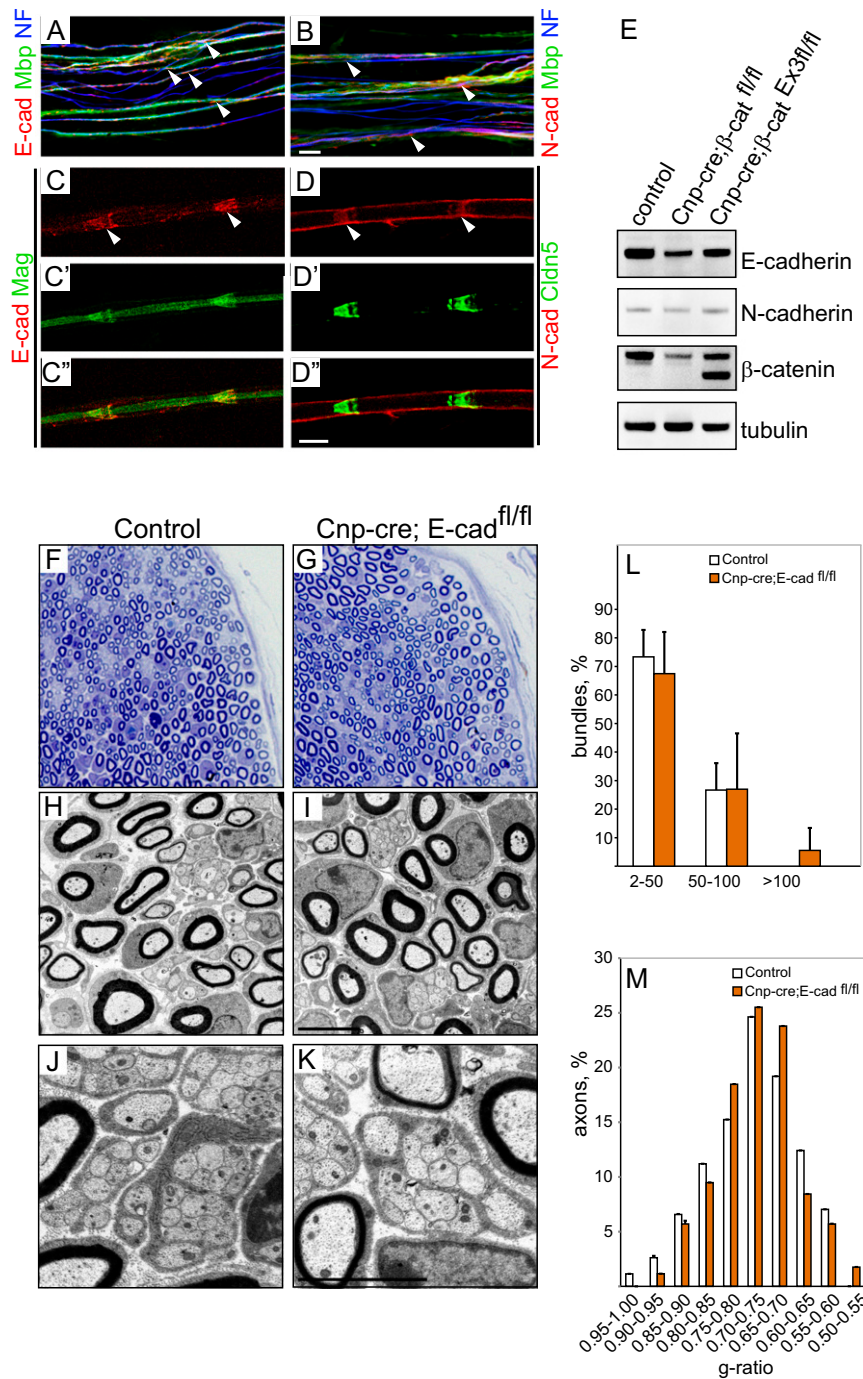


Fig. 56. Analysis of the adherens junction components E-cadherin and N-cadherin, during SC development. (A and B) At P3, E-cadherin localized in a punctate pattern along the myelinating fibers, whereas a very low level of N-cadherin was dispersed along the myelinating fibers, as assessed by immunostaining for E-cadherin or N-cadherin (red), myelin basic protein (MBP) (green), and Neurofilament (blue). (C–D) In adult mice, both E-cadherin and N-cadherin were localized to the noncompact myelin regions, e.g., Schmidt–Lantermann incisures (SLIs), which contain adherens junctions, as shown by coimmunolabeling with antibodies against E-cadherin or N-cadherin (red) and SLI markers Mag or Cldn5 (green). (E) Amounts of E-cadherin and N-cadherin in the Cnp-cre; β-catenin LOF and GOF mutant sciatic nerves, as determined by a Western blot using antibodies against E-cadherin, N-cadherin, β-catenin, and α-tubulin, as a loading control. N-cadherin levels were not changed, whereas E-cadherin appeared reduced in both LOF and GOF mutant mice compared with the controls. (F and G) Transverse semithin sections and (H–K) electron micrographs of the peripheral nerves of control and Cnp-cre; E-cad^{fl/fl} mutant mice. Quantifications of the (L) axonal bundle sizes and (M) g ratios, which were determined from electron micrographs, show no significant difference between control and Cnp-cre; E-cad^{fl/fl} mutant mice. Error bars indicate SD (*n* = 3). (Scale bars: 10 μm in F–I and 5 μm in J and K.)

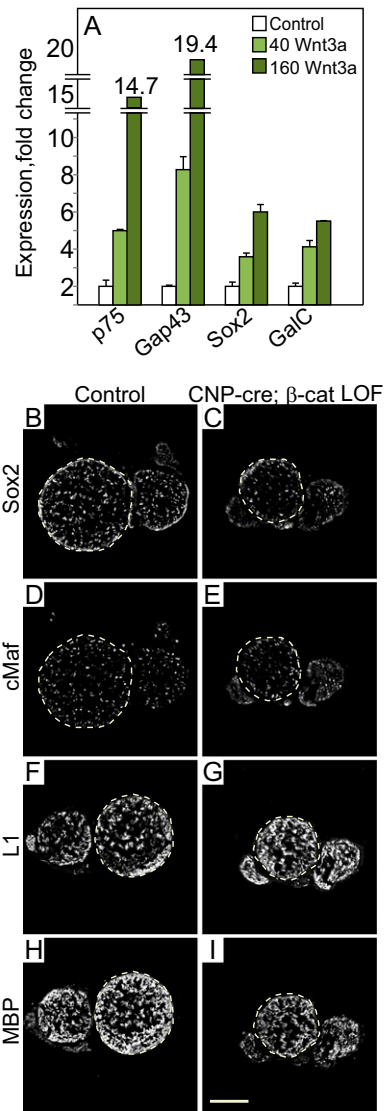


Fig. S7. Gene expression signature imposed by canonical Wnt ligands *in vitro* and by β -catenin LOF mutations *in vivo*. **(A)** Wnt3a induces up-regulation of p75, Gap43, Sox2, and GalC in a dose-dependent manner. Induction of a set of indicated genes by 40 and 160 ng/mL Wnt3a in primary SCs occurs similarly to Chir98014 treatment. Error bars indicate SD calculated from three independent primary cell batches. **(B–I)** Immunostainings on transverse sections of the sciatic nerves of **(B, D, F, and H)** control and **(C, E, G, and I)** *Cnp-cre;* β -catenin^{fl/fl} mice using antibodies against MBP, L1, cMaf, and Sox2. Dotted outlines surround axons. (Scale bar: 100 μ m.)

Table S1. Expression of ligands and receptors of Wnt signaling in neurons and SCs during development

	Neurons*			SCs†		
	E12.5	E14.5	E17.5	E12.5	E14.5	E17.5
Wnt1	—	—	—	—	—	—
Wnt2	+	+	+	—	+	+
Wnt2b	—	—	—	—	—	—
Wnt3	—	—	—	—	—	—
Wnt3a	—	—	—	—	—	—
Wnt5a	—	—	—	—	—	—
Wnt5b	—	—	—	—	—	—
Wnt6	+	+	+	—	—	—
Wnt9b	+	+	+	—	—	—
Wnt11	—	—	—	—	—	—
Rspo1	+	+	+	—	—	—
Rspo2	+	+	+	—	—	—
Rspo3	+	+	+	—	—	—
Rspo4	+	+	+	—	—	—
Fzd1	—	+	+	—	+	+
Fzd2	—	+	+	—	+	+
Fzd3	+	+	+	+	+	+
Fzd4	—	—	+	—	—	—
Fzd5	—	—	—	—	—	—
Fzd6	—	—	—	—	—	—
Fzd7	+	+	+	+	+	+
Fzd8	+	+	+	+	+	+
Fzd9	—	—	+	—	—	+
Fzd10	—	—	—	—	—	—
Lgr4	n.a.	n.a.	n.a.	+	+	+
Lgr5	n.a.	n.a.	n.a.	+	+	+
Lgr6	n.a.	n.a.	n.a.	+	+	+

+, expression detected; —, no expression detected; n.a., not analyzed.

*Expression in cell bodies of peripheral neurons of dorsal root ganglia determined by immunohistochemistry (Fig. 1A).

†Expression in SCs along spinal and sciatic nerves determined by immunohistochemistry and real-time PCR (Fig. 1 A and B).

Table S2. Gene enrichment by GO and PANTHER classification of genes significantly down-regulated upon β -catenin LOF and up-regulated upon β -catenin GOF mutations

Term	%	Genes	Fold enrichment
GO:0043209~myelin sheath	2.7	SERINC5, TUBB4	63.9
BP00280:Lysosome transport	2.7	LAMP1, CTSA	45
GO:0001505~regulation of neurotransmitter levels	4	SYN1, ABAT, CLN8	12
GO:0016055~Wnt receptor signaling pathway	6.7	TCF7, NKD1, WISP1, FZD3, AXIN2	9.6
MF00270:Membrane traffic regulatory protein	4	LAMP1, SYN1, BIN1	8.9
GO:0006979~response to oxidative stress	4	NQO1, CLN8, SRXN1	8.6
GO:0007611~learning or memory	4	ITGA5, PRKAR1B, CLN8	8.4
GO:0019226~transmission of nerve impulse	6.7	SERINC5, SYN1, FYN, ABAT, CLN8	5.5
GO:0042803~protein homodimerization activity	5.3	MTMR2, PTPRE, LOC100043986, C630004H02RIK, ABAT	5
GO:0005773~vacuole	5.3	MTMR2, LAMP1, CTSA, CLCN7	5
MF00261:Actin binding cytoskeletal protein	6.7	ARPC1A, LIMS2, SYN1, MYL1, TMOD1	4.4
BP00122:Ligand-mediated signaling	6.7	FGF5, AHRR, WISP1, CLCF1, IL6RA	3.8
GO:0046983~protein dimerization activity	6.7	MTMR2, PTPRE, SYN1, LOC100043986, C630004H02RIK, ABAT	3.6
GO:0008092~cytoskeletal protein binding	8	ARPC1A, SYN1, FYN, AFAP1, FEZ1, TMOD1	3.5
GO:0007154~cell communication	8	SERINC5, SYN1, FYN, GJA1, ABAT, CLN8	3.3
GO:0007399~nervous system development	14.7	EFHD1, FGF5, TCF7, SERINC5, SOCS2, FYN, LOC100043986, C630004H02RIK, GJA1, FZD3, SDF4, CLN8	3.2
GO:0022008~neurogenesis	9.3	EFHD1, FGF5, SOCS2, FYN, LOC100043986, C630004H02RIK, GJA1, CLN8	3.2
GO:0048699~generation of neurons	8	EFHD1, SOCS2, FYN, LOC100043986, C630004H02RIK, GJA1, CLN8	3
BP00111:Intracellular signaling cascade	10.7	FGF5, STAC2, SOCS2, FYN, RAB34, LOC100047353, SDF4, IL6RA	2.6
BP00125:Intracellular protein traffic	10.7	MTMR2, LAMP1, SYN1, RAB34, DNAJC6, CTSA, BIN1, TUBB4	2.4
BP00274:Cell communication	12	FGF5, AHRR, PCDH1, PTPRE, STAC2, WISP1, CLCF1, TGFBI, IL6RA	2.2
GO:0030154~cell differentiation	16	FGF5, NKD1, SOCS2, C630004H02RIK, GJA1, EFHD1, FYN, CLCF1, LOC100043986, BIN1, CLN8, SDF4, TMOD1	1.9
GO:0005737~cytoplasm	49.3	GNPTG, EXTL3, NKD1, 1500015010RIK, GJA1, CRCP, CTSA, OGDH, TSC22D1, MTMR2, EFHD1, SERINC5, AHRR, SYN1, ERAP1, GPSM2, LOC100047353, AXIN2, NQO1, MAP2K7, AFAP1, SDF4, ST6GAL1, C630004H02RIK, CDKL2, ARPC1A, LAMP1, FYN, PRKAR1B, RAB34, LOC100043986, ABAT, BIN1, CLCN7, CLN8, SRXN1, FEZ1, TMOD1	1.5
GO:0044444~cytoplasmic part	32	GNPTG, ST6GAL1, EXTL3, 1500015010RIK, GJA1, CRCP, CTSA, OGDH, MTMR2, LAMP1, EFHD1, SERINC5, SYN1, FYN, RAB34, ABAT, GPSM2, ERAP1, CLCN7, CLN8, SDF4, SRXN1, FEZ1, TMOD1	1.5
GO:0005515~protein binding	44	GNPTG, FGF5, NKD1, GJA1, RTKN, CTSA, MTMR2, PCDH1, WISP1, SYN1, CLCF1, TGFBI, DNAJC6, LOC100047353, ERAP1, AXIN2, AFAP1, MAP2K7, PTPRE, SOCS2, C630004H02RIK, FZD3, IL6RA, ARPC1A, LAMP1, CRCT1, ITGA5, FYN, LOC100043986, ABAT, BIN1, CLCN7, FEZ1, TMOD1	1.4

GO, Gene Ontology; PANTHER, Protein Analysis Through Evolutionary Relationships. $P < 0.05$.

Table S3. Gene enrichment by GO and PANTHER classification of genes significantly deregulated upon β -catenin GOF mutations

Term	%	Genes	Fold Enrichment
		Up-regulated genes	
GO:0016416~O-palmitoyltransferase activity	1.1	CPT1C, CPT2	54.9
GO:0031099~regeneration	1.6	NINJ1, GAP43, PLG	14.7
GO:0007266~Rho protein signal transduction	1.6	BCL6, TAX1BP3, CDC42EP5	12.5
GO:0007265~Ras protein signal transduction	2.2	RRAS2, BCL6, TAX1BP3, CDC42EP5	7.7
GO:0043087~regulation of GTPase activity	2.7	TBC1D25, GDI1, SMAP2, TBC1D9, BCL6	6.1
GO:0051188~cofactor biosynthetic process	2.2	GSS, COQ4, MOCS2, COQ9	5.0
GO:0019318~hexose metabolic process	3.3	PHKA2, GALM, ATF3, ENO2, PFKP, PMM2	4.0
GO:0006732~coenzyme metabolic process	2.7	GSS, COQ4, SDHB, MOCS2, COQ9	3.9
GO:0046578~regulation of Ras protein signal transduction	3.3	TBC1D25, PLEKHG3, SMAP2, TBC1D9, BCL6, NET1	3.7
GO:0003712~transcription cofactor activity	3.3	NRBF2, SQSTM1, SRA1, TLE1, HES6, DAXX	3.7
GO:0022603~regulation of anatomical structure morphogenesis	3.3	AGGF1, SEMA4F, NGFR, RUNX2, PLG, CDC42EP5	3.6
GO:0005773~vacuole	3.8	CTS2, GABARAP1, LAPTM5, GLA, 0610031J06RIK, VPS11, GABARAP	3.6
GO:0005667~transcription factor complex	4.3	FOS, NRBF2, ATF3, SRA1, TLE1, PAX3, HES6, RUNX2	3.6
BP00276:General vesicle transport	3.8	GDI1, SRA1, AP3B2, BET1L, GOSR2, RAB21, AP3B1	3.6
GO:0005996~monosaccharide metabolic process	3.3	PHKA2, GALM, ATF3, ENO2, PFKP, PMM2	3.5
GO:0005764~lysosome	3.3	CTS2, LAPTM5, GLA, 0610031J06RIK, VPS11, GABARAP	3.5
GO:0005083~small GTPase regulator activity	3.8	TBC1D25, GDI1, PLEKHG3, SMAP2, TBC1D9, NET1, ARHGAP10	3.4
MF00126:Dehydrogenase	3.3	SDHB, NDUFB7, ALDH1B1, HSD17B3, ACADL, RETSAT	3.3
GO:0044431~Golgi apparatus part	3.8	ST8SIA4, AP3B2, BET1L, GOSR2, GABARAP, RAB21, AP3B1	3.2
GO:0016564~transcription repressor activity	3.3	ATF3, BCL6, TLE1, PAX3, SCMH1, DAXX	3.1
GO:0051093~negative regulation of developmental process	3.3	ZFP36, SEMA4F, BCL6, NGFR, SMURF1, PLG	3.0
GO:0032787~monocarboxylic acid metabolic process	3.8	CPT1C, ATF3, CPT2, PEX5, ACADL, RNPEP, NR1H4	2.9
GO:0009898~internal side of plasma membrane	4.3	PHKA2, CADPS, RRAS2, AP3B2, HGS, VPS11, GAP43, AP3B1	2.9
GO:0008284~positive regulation of cell proliferation	3.8	AGGF1, SPHK2, TICAM1, BCL6, PAX3, NGFR, RUNX2	2.8
GO:0050790~regulation of catalytic activity	6.0	TBC1D25, GDI1, SMAP2, GLA, SPHK2, TSC1, TBC1D9, IKBKG, BCL6, GADD45B, AVPI1	2.7
GO:0008134~transcription factor binding	3.8	NRBF2, SQSTM1, SRA1, TLE1, HES6, DAXX, NR1H4	2.7
GO:0009966~regulation of signal transduction	8.2	TBC1D9, TAX1BP3, PRDX1, AVPI1, TBC1D25, PLEKHG3, DKK3, SMAP2, SQSTM1, TICAM1, IKBKG, BCL6, NGFR, RUNX2, NET1	2.6
GO:0005975~carbohydrate metabolic process	5.4	PHKA2, GALM, ATF3, GLA, ST8SIA4, ENO2, PFKP, ITIH5, GLB1L2, PMM2	2.5
GO:0015031~protein transport	7.6	GDI1, PEX5, NAPA, GABARAP, CADPS, PLEKHA8, AP3B2, BET1L, EXOC3, HGS, GOSR2, VPS11, RAB21, AP3B1	2.4
GO:0045184~establishment of protein localization	7.6	GDI1, PEX5, NAPA, GABARAP, CADPS, PLEKHA8, AP3B2, BET1L, EXOC3, HGS, GOSR2, VPS11, RAB21, AP3B1	2.4
GO:0044255~cellular lipid metabolic process	5.4	CPT1C, CPT2, GLA, SPHK2, PEX5, PLA2G2C, PI4KB, ACADL, RNPEP, RETSAT	2.3
GO:0008104~protein localization	8.2	GDI1, PEX5, NAPA, GABARAP, CADPS, PLEKHA8, AP3B2, BET1L, EXOC3, HGS, BCL6, GOSR2, VPS11, RAB21, AP3B1	2.2
GO:0010646~regulation of cell communication	8.2	TBC1D9, TAX1BP3, PRDX1, AVPI1, TBC1D25, PLEKHG3, DKK3, SMAP2, SQSTM1, TICAM1, IKBKG, BCL6, NGFR, RUNX2, NET1	2.2
GO:0050793~regulation of developmental process	6.0	ZFP36, AGGF1, SEMA4F, BCL6, NGFR, E4F1, SMURF1, RUNX2, PLG, CDC42EP5, AP3B1	2.2
GO:0009888~tissue development	6.5	NRTN, GLA, TSC1, TNFRSF19, NINJ1, PAX3, KRT4, NGFR, GPNMB, RUNX2, GAP43, PLG	2.1

Table S3. Cont.

Term	%	Genes	Fold Enrichment
GO:0031090~organelle membrane	8.7	CPT1C, CPT2, NDUFB7, PEX5, PI4KB, GABARAP, PEX11A, SLC17A8, SDHB, SLC25A14, LAPTM5, ST8SIA4, BET1L, GOSR2, RAB21, RETSAT	2.1
GO:0006629~lipid metabolic process	6.5	CPT1C, CPT2, GLA, SPHK2, PEX5, PLA2G2C, HSD17B3, PI4KB, ACADL, RNPEP, NR1H4, RETSAT	1.9
GO:0007242~intracellular signaling cascade	8.2	ZFP36, GDI1, PI4KB, TAX1BP3, DAXX, AVPI1, PLEKHG3, DOK5, RRAS2, IKKKG, BCL6, GADD45B, RAB21, NET1, CDC42EP5	1.8
GO:0030528~transcription regulator activity	10.3	NRBF2, TCFAP2B, SRA1, TLE1, PAX3, HES6, 2210012G02RIK, TAX1BP3, DAXX, FOS, MAX, ATF3, SQSTM1, SERTAD3, BCL6, E4F1, SCMH1, RUNX2, NR1H4	1.7
GO:0048519~negative regulation of biological process	10.3	ZFP36, SPHK2, TLE1, PAX3, TAX1BP3, DAXX, PLG, DKK3, AKT1S1, TSC1, GLA, SEMA4F, SERTAD3, BCL6, KRT4, SMURF1, NGFR, SCMH1, RUNX2	1.6
GO:0030154~cell differentiation	12.0	NRTN, SRA1, PEX5, ANPEP, NAPA, HES6, PAX3, PLG, PEX11A, TSC1, AGGF1, SQSTM1, SEMA4F, SEMA4B, BCL6, KRT4, SMURF1, NGFR, GPNMB, GADD45B, RUNX2, GAP43	1.6
GO:0005737~cytoplasm	48.9	CPT2, SYT5, TOLLIP, ESD, LOC100046081, PEX5, FLCN, PRDX1, DAXX, SMAP2, CLK3, NUBP2, LACE1, AP3B2, SERTAD3, E4F1, VPS11, ATP6V0D1, RAB21, NET1, AP3B1, ZFP36, CTSZ, SGK1, MPP1, GTPBP8, PFKP, 0610031J06RIK, TLE1, COQ9, PI4KB, DCTN3, ACADL, PMM2, COQ4, PRUNE, AA467197, ALDH1B1, PSME3, NGFR, BIVM, NDUFB7, DUSP10, NAPA, NAGPA, GALM, THTPA, LAPTM5, AKT1S1, TUBGCP5, 1700029P11RIK, AGGF1, SQSTM1, ENO2, HSPE1, LYPLAL1, GPNMB, RUNX2, CDC42EP5, DTNA, CPT1C, GDI1, GABARAPL1, NRBF2, MOCS2, SPHK2, SRA1, BAALC, DRG2, MRRF, TAX1BP3, TPBG, GABARAP, CADPS, PEX11A, SLC17A8, SDHB, SLC25A14, PLEKHA8, GLA, INVS, TSC1, ST8SIA4, IKKKG, BET1L, HGS, GOSR2, OGG1, ARHGAP10, RETSAT	1.5
GO:0044424~intracellular part	58.7	SYT5, LOC100046081, FLCN, ZFP87, CLK3, RAB21, NET1, TCFAP2B, GTPBP8, TOR1AIP1, HES6, DCTN3, BIVM, DUSP10, NAPA, THTPA, GALM, AKT1S1, LAPTM5, AGGF1, HSPE1, RUNX2, NR1H4, CDC42EP5, GABARAPL1, NRBF2, MOCS2, SPHK2, SRA1, 2210012G02RIK, TAX1BP3, MRRF, TPBG, SLC25A14, ATF3, PLEKHA8, TSC1, ST8SIA4, IKKKG, HGS, BET1L, GOSR2, SCMH1, ARHGAP10, CPT2, TOLLIP, ESD, PEX5, PAX3, PRDX1, DAXX, MAX, FOS, SMAP2, NUBP2, FRMD8, LACE1, SERTAD3, AP3B2, E4F1, VPS11, ATP6V0D1, AP3B1, ZFP36, CTSZ, SGK1, MPP1, PFKP, 0610031J06RIK, COQ9, TLE1, PI4KB, ACADL, PMM2, COQ4, PRUNE, AA467197, ALDH1B1, PSME3, NGFR, GADD45B, WIZ, NDUFB7, NAGPA, 1700029P11RIK, TUBGCP5, SQSTM1, TRP53INP2, ENO2, BCL6, KRT4, LYPLAL1, GPNMB, DTNA, CPT1C, GDI1, BAALC, DRG2, GABARAP, CADPS, PEX11A, SDHB, SLC17A8, GLA, INVS, OGG1, CYPT9, RETSAT	1.2
GO:0043231~intracellular membrane-bounded organelle	44.0	CPT2, SYT5, ESD, PEX5, PAX3, PRDX1, DAXX, ZFP87, MAX, FOS, CLK3, NUBP2, LACE1, AP3B2, SERTAD3, E4F1, VPS11, ATP6V0D1, RAB21, NET1, AP3B1, ZFP36, CTSZ, SGK1, TCFAP2B, GTPBP8, TOR1AIP1, 0610031J06RIK, TLE1, COQ9, PI4KB, HES6, ACADL, COQ4, PRUNE, AA467197, ALDH1B1, PSME3, NGFR, BIVM, GADD45B, WIZ, NDUFB7, DUSP10, NAPA, NAGPA, LAPTM5, 1700029P11RIK, SQSTM1, TRP53INP2, BCL6, HSPE1, GPNMB, RUNX2, NR1H4, CPT1C, GABARAPL1, NRBF2, SRA1, 2210012G02RIK, DRG2, MRRF, TAX1BP3, TPBG, GABARAP, PEX11A, SLC17A8, SDHB, SLC25A14, ATF3, GLA, INVS, ST8SIA4, IKKKG, BET1L, HGS, GOSR2, SCMH1, OGG1, CYPT9, RETSAT	1.2

Table S3. Cont.

Term	%	Genes	Fold Enrichment
		Down-regulated genes	
GO:0006270~DNA replication initiation	2.6	CCNE2, MCM7, MCM3, MCM5	47.0
GO:0006284~base-excision repair	2.0	HMGB2, UNG, POLD1	18.6
GO:0008376~acetylgalactosaminyltransferase activity	2.0	CSGALNACT1, GALNT1, GALNT10	12.3
GO:0005913~cell-cell adherens junction	2.0	PVRL3, ABI2, CTNNA1	11.7
GO:0003725~double-stranded RNA binding	2.0	DHX9, ADARB1, TLR3	10.9
MF00063:Histone	2.0	HIST1H2AG, HIST2H2AC, HIST1H2AD, HIST1H2AH, HIST1H2AK	9.1
MF00243:DNA helicase	2.6	MCM7, POLQ, MCM3, MCM5	8.4
GO:0042770~DNA damage response, signal transduction	2.6	MSH6, UACA, HUS1, BRCA1	8.2
GO:0000793~condensed chromosome	4.0	RPA1, HMGB2, CBX3, NUP85, BRCA1, NCAPD3	6.8
GO:0006334~nucleosome assembly	2.6	HIST1H2AG, HIST2H2AC, HIST1H2AD, HIST1H2AH, HIST1H2AK, ASF1B	6.4
GO:0006310~DNA recombination	2.6	RPA1, MSH6, UNG, HUS1	6.3
GO:0000785~chromatin	5.3	MSH6, HMGN3, HIST1H2AG, HIST2H2AC, HIST1H2AD, DNMT1, HIST1H2AH, CBX3, HIST1H2AK, ASF1B	5.9
GO:0006323~DNA packaging	3.3	HIST1H2AG, HIST2H2AC, HIST1H2AD, HIST1H2AH, HIST1H2AK, ASF1B, NCAPD3	5.8
GO:0006974~response to DNA damage stimulus	9.3	CLSPN, MSH6, HMGB2, DTL, UNG, HUS1, BRCA1, FANCL, RPA1, UACA, TIMELESS, POLD1, POLQ, FANCC	5.7
GO:0006259~DNA metabolic process	11.9	MSH6, CDC6, CLSPN, HMGB2, DTL, UNG, HUS1, MCM3, MCM5, BRCA1, RPA1, FANCL, CCNE2, MCM7, POLD1, DNMT1, POLQ, FANCC	5.0
GO:0008194~UDP-glycosyltransferase activity	2.6	CSGALNACT1, B3GAT1, GALNT1, GALNT10	5.0
GO:0033554~cellular response to stress	9.9	DHX9, CLSPN, MSH6, HMGB2, DTL, UNG, HUS1, BRCA1, FANCL, RPA1, UACA, TIMELESS, POLD1, POLQ, FANCC	4.4
GO:0005635~nuclear envelope	3.3	FANCL, UACA, LMNB1, CBX3, NUP85	4.0
GO:0003682~chromatin binding	3.3	RPA1, MSH6, CDC6, HMGN3, CBX3	4.0
MF00100:G protein modulator	6.0	DLC1, RASSF4, LOC100045542, ARHGEF6, RUNDC3B, ABI2, IQGAP2, ARHGAP12, EHD4	3.6
GO:0007049~cell cycle	11.3	CDC6, CLSPN, E2F2, RBL1, 1190002H23RIK, SKP2, ANLN, MCM3, NCAPD3, BRCA1, MLF1, RPA1, CCNE2, RASSF4, MCM7, TIMELESS, G0S2	3.3
MF00178:Extracellular matrix	5.3	LINGO4, 1200009O22RIK, TLR3, COL12A1, LRIG3, MMP15, MEGF10, OTOA	3.3
GO:0051276~chromosome organization	7.3	HIST1H2AG, HIST1H2AD, RBL1, HAT1, CBX3, NCAPD3, RPA1, PHF17, HIST2H2AC, HIST1H2AH, DNMT1, HIST1H2AK, ASF1B	3.2
GO:0016568~chromatin modification	4.0	PHF17, RBL1, DNMT1, CBX3, HAT1, ASF1B	3.0
GO:0006996~organelle organization	16.6	RHOJ, DLC1, HMGB2, TYRP1, ATL2, HIST1H2AG, HIST1H2AD, HAT1, CBX3, ANLN, RPA1, TFAM, FXN, HIST2H2AC, ASF1B, CDC6, RBL1, SIRPA, NCAPD3, BRCA1, ZDHHC15, MAN2A1, PHF17, TIMELESS, HIST1H2AH, DNMT1, HIST1H2AK	2.7
GO:0045934~negative regulation of nucleobase, nucleoside, nucleotide and nucleic acid metabolic process	6.0	MSH6, CLSPN, TIMELESS, HUS1, RBL1, DNMT1, CBX3, HAT1, ZFH3	2.7
GO:0031327~negative regulation of cellular biosynthetic process	6.0	CLSPN, TIMELESS, HUS1, RBL1, DNMT1, CBX3, HAT1, ZFH3, BRCA1	2.5
GO:0022402~cell cycle process	5.3	RPA1, CDC6, TIMELESS, SKP2, ANLN, BRCA1, NCAPD3, MLF1	2.4
GO:0010605~negative regulation of macromolecule metabolic process	6.6	MSH6, CLSPN, TIMELESS, HUS1, RBL1, SKP2, DNMT1, CBX3, HAT1, ZFH3	2.3
GO:0006464~protein modification process	12.6	PTPRB, GALNT1, HUS1, PASK, SKP2, HAT1, ABI2, TTL1, CAMKK2, ZDHHC15, MAN2A1, PHF17, EPHA7, GALNT10, SIAH1B, PRKACA, ASPH, MAP2K6, DUSP6	1.8
GO:0006950~response to stress	11.3	BATS, MSH6, DHX9, CLSPN, HMGB2, DTL, UNG, HUS1, TLR3, BRCA1, RPA1, FANCL, UACA, TIMELESS, POLD1, POLQ, FANCC	1.7
GO:0006139~nucleobase, nucleoside, nucleotide and nucleic acid metabolic process	27.2	E2F2, CLSPN, HMGB2, UNG, HUS1, CBX3, MYBL2, DMRTA1, MLF1, CCNE2, RPA1, MTHFD1, FANCL, TFAM, MCM7, HOXA5, PSIP1, ETV1, ASF1B, POLQ, SFRS14, FANCC, CDC6, MSH6, ADARB1, IKZF2, DTL, RBL1, SSB, AK5, MCM3, BRCA1, MCM5, CSGALNACT1, HOXB3, PHF17, MED30, TIMELESS, POLD1, DNMT1, ZFH3	1.7

Table S3. Cont.

Term	%	Genes	Fold Enrichment
GO:0044260~cellular macromolecule metabolic process	41.1	CLSPN, E2F2, PASK, DNAJC10, CBX3, TTLL1, DMRTA1, CAMKK2, CCNE2, FANCL, MCM7, FBXO28, PSIP1, PRKACA, ASPH, MAP2K6, FANCC, CDC6, CALR4, DTL, RBL1, SKP2, MCM3, MCM5, ZDHHC15, MAN2A1, TIMELESS, SIAH1B, KLHL13, HMGB2, GALNT1, UNG, HUS1, ABI2, HAT1, MYBL2, MLF1, RPA1, TFAM, CYLD, GALNT10, HOXA5, ETV1, ASF1B, POLQ, SFRS14, PTPRB, MSH6, ADARB1, IKZF2, SSB, BRCA1, HOXB3, CSGALNACT1, PHF17, EPHA7, MED30, POLD1, SPCS3, DNMT1, ZFH3, DUSP6	1.6
GO:0034641~cellular nitrogen compound metabolic process	27.8	E2F2, CLSPN, HMGB2, TYRP1, UNG, HUS1, CBX3, MYBL2, DMRTA1, MLF1, FANCL, CCNE2, RPA1, MTHFD1, TFAM, MCM7, HOXA5, PSIP1, ETV1, ASF1B, POLQ, SFRS14, FANCC, CDC6, MSH6, ADARB1, IKZF2, DTL, RBL1, SSB, AK5, MCM3, BRCA1, MCM5, CSGALNACT1, HOXB3, PHF17, MED30, TIMELESS, POLD1, DNMT1, ZFH3	1.6
GO:0044267~cellular protein metabolic process	18.5	GALNT1, PASK, HUS1, DNAJC10, ABI2, HAT1, TTLL1, CAMKK2, FANCL, CYLD, GALNT10, FBXO28, PRKACA, ASPH, MAP2K6, PTPRB, CALR4, DTL, SKP2, BRCA1, ZDHHC15, MAN2A1, PHF17, EPHA7, SIAH1B, SPCS3, KLHL13, DUSP6	1.6
GO:0006807~nitrogen compound metabolic process	27.8	E2F2, CLSPN, HMGB2, TYRP1, UNG, HUS1, CBX3, MYBL2, DMRTA1, MLF1, FANCL, CCNE2, RPA1, MTHFD1, TFAM, MCM7, HOXA5, PSIP1, ETV1, ASF1B, POLQ, SFRS14, FANCC, CDC6, MSH6, ADARB1, IKZF2, DTL, RBL1, SSB, AK5, MCM3, BRCA1, MCM5, CSGALNACT1, HOXB3, PHF17, MED30, TIMELESS, POLD1, DNMT1, ZFH3	1.5
GO:0009058~biosynthetic process	25.2	E2F2, TYRP1, GALNT1, CBX3, MYBL2, DMRTA1, MLF1, RPA1, CCNE2, MTHFD1, CYLD, TFAM, MCM7, GALNT10, FXN, HOXA5, PSIP1, ETV1, ASF1B, POLQ, CDC6, IKZF2, DTL, RBL1, MCM3, BRCA1, MCM5, ZDHHC15, CSGALNACT1, HOXB3, PHF17, MAN2A1, MED30, TIMELESS, POLD1, DNMT1, ZFH3, GPAM	1.5
GO:0005515~protein binding	45.7	RHOJ, DLC1, BAT5, CLSPN, E2F2, 1200009022RIK, ATLL2, DNAJC10, CBX3, TLR3, IQGAP2, MEGF10, ARHGAP12, CAMKK2, FANCL, MCM7, PACSIN2, SYNJ2, COL12A1, KLHL21, PRKACA, MAP2K6, LOC100045542, CALR4, 1190002H23RIK, RBL1, SKP2, G3BP2, MPP6, USHBP1, NUP85, PCDH7, CTNNA1, SIRPA, PRL3D1, LRCH1, TIMELESS, SIAH1B, PYGO1, KLHL13, PYGO2, ADAM12, SNX18, HMGB2, TYRP1, ABI2, HAT1, ANLN, LRIG3, MLF1, CYLD, LINGO4, PVRL3, SNX24, ASF1B, EHD4, CNKSR2, IKZF2, ITGA2, CENPK, BRCA1, KCTD7, PHF17, RASSF4, EPHA7, MED30, UACA, DNMT1, DUSP6	1.5
GO:0044237~cellular metabolic process	47.0	CLSPN, E2F2, PASK, DNAJC10, CBX3, TTLL1, DMRTA1, CAMKK2, FANCL, MTHFD1, CCNE2, MCM7, FXN, FBXO28, PSIP1, SYNJ2, PRKACA, ASPH, MAP2K6, FANCC, CDC6, PCYOX1L, CALR4, DTL, RBL1, SKP2, MCM3, MCM5, ZDHHC15, MAN2A1, TIMELESS, SIAH1B, KLHL13, GPAM, HMGB2, TYRP1, GALNT1, UNG, HUS1, ABI2, HAT1, MYBL2, MLF1, CYB561D2, RPA1, TFAM, CYLD, GALNT10, HOXA5, ETV1, POLQ, ASF1B, SFRS14, PTPRB, LPL, MSH6, ADARB1, IKZF2, AK5, SSB, BRCA1, HOXB3, CSGALNACT1, PHF17, EPHA7, MED30, POLD1, SPCS3, DNMT1, ZFH3, DUSP6	1.4
GO:0043229~intracellular organelle	57.0	E2F2, CLSPN, HMGN3, ATLL2, CTDSP1, RUSC1, DNAJC10, CBX3, TLR3, RHOX4E, TTLL1, DMRTA1, FANCL, CCNE2, MTHFD1, MCM7, FXN, PACSIN2, HIST2H2AC, PSIP1, SLC25A27, PRKACA, ASPH, FANCC, CDC6, LOC100045542, CALR4, DTL, MYCT1, 1190002H23RIK, RBL1, NUP85, MCM3, CTNNA1, MCM5, NCAPD3, MAN2A1, TIMELESS, SIAH1B, PYGO1, PYGO2, GPAM, PACS1, HMGB2, GALNT1, TYRP1, LMNB1, HIST1H2AG, UNG, HIST1H2AD, HUS1, ABI2, HAT1, ANLN, MYBL2, MLF1, RPA1, TFAM, CYLD, GALNT10, HOXA5, ETV1, ASF1B, SFRS14, EHD4, MSH6, DHX9, ICA1, ADARB1, IKZF2, CEP135, SSB, DONSON, CENPK, BRCA1, HOXB3, CSGALNACT1, B3GAT1, PHF17, MED30, UACA, POLD1, 5033414D02RIK, SPCS3, HIST1H2AH, DNMT1, HIST1H2AK, ZFH3	1.3

Table S3. Cont.

Term	%	Genes	Fold Enrichment
GO:0005622~intracellular	66.2	BAT5, DLC1, HMG3, CTDSPL, RUSC1, PASK, CBX3, TLR3, IQGAP2, PACSIN2, PSIP1, PRKACA, SLC25A27, ASPH, LOC100045542, CALR4, DTL, RBL1, SKP2, CTNNA1, NCAPD3, TIMELESS, SIAH1B, PYGO1, PYGO2, PACS1, HMGB2, LMNB1, HUS1, ANLN, MYBL2, HOXA5, ASF1B, SFRS14, CNKSR2, DHX9, IKZF2, SSB, AK5, DONSON, BRCA1, HOXB3, B3GAT1, UACA, POLD1, SPCS3, DNMT1, ZFH3, RHOJ, E2F2, CLSPN, ATL2, DNAJC10, RHOX4E, TLL1, DMRTA1, ARHGAP12, CAMKK2, CCNE2, MTHFD1, FANCL, MCM7, FXN, HIST2H2AC, SYNJ2, FANCC, CDC6, MYCT1, ARHGEF6, 1190002H23RIK, G3BP2, NUP85, MCM3, MCM5, MAN2A1, GPAM, TYRP1, GALNT1, HIST1H2AG, UNG, HIST1H2AD, ABI2, HAT1, MLF1, RPA1, CYLD, TFAM, GALNT10, ETV1, EHD4, MSH6, ICA1, ADARB1, CEP135, CENPK, CSGALNACT1, PHF17, MED30, 5033414D02RIK, HIST1H2AH, HIST1H2AK, DUSP6	1.2
GO:0005488~binding	72.2	BAT5, DLC1, HMG3, 1200009O22RIK, PASK, CBX3, TLR3, IQGAP2, MEGF10, ACBD4, PACSIN2, PSIP1, COL12A1, SLC25A27, PRKACA, ASPH, MAP2K6, LOC100045542, CALR4, RBL1, SKP2, USHBP1, CTNNA1, SIRPA, NCAPD3, TIMELESS, LRCH1, SIAH1B, PYGO1, PYGO2, HMGB2, ANLN, LRIG3, MYBL2, HOXA5, PVRL3, POLQ, ASF1B, SFRS14, CNKSR2, LPL, DHX9, IKZF2, ITGA2, SSB, AK5, BRCA1, KCTD7, HOXB3, B3GAT1, EPHA7, UACA, POLD1, DNMT1, ZFH3, RHOJ, E2F2, CLSPN, ATL2, DNAJC10, RHOX4E, DMRTA1, ARHGAP12, CAMKK2, FANCL, MTHFD1, MCM7, HIST2H2AC, KLHL21, SYNJ2, CDC6, 1190002H23RIK, G3BP2, MPP6, NUP85, MMP15, PCDH7, MCM3, MCM5, ZDHHC15, MAN2A1, PRL3D1, KLHL13, ADAM12, SNX18, TYRP1, GALNT1, HIST1H2AG, HIST1H2AD, ABI2, HAT1, MLF1, CYB561D2, RPA1, CYLD, TFAM, LINGO4, GALNT10, ETV1, SNX24, EHD4, MSH6, ADARB1, CENPK, CSGALNACT1, RASSF4, PHF17, MED30, HIST1H2AH, HIST1H2AK, DUSP6	1.2

$P < 0.05$.